Nuclear magnetic resonance investigations of calcium-antagonist drugs. Part 4. Conformational and dynamic features of nicardipine {methyl 2-[methyl(phenylmethyl)amino]ethyl 1,4-dihydro-2,6-dimethyl-4-(3-nitrophenyl)pyridine-3,5-dicarboxylate} in deuterium oxide

Luigi Calzolai, Elena Gaggelli, Antonella Maccotta and Gianni Valensin

Department of Chemistry, University of Siena, Pian dei Mantellini 44, Siena 53100, Italy

Conformation and dynamics of nicardipine in deuterium oxide were investigated by ^{1}H and ^{13}C NMR spectroscopy. Molecular motions were characterised by effective correlation times calculated by ^{13}C spin–lattice relaxation rates and verified by the frequency dependence of ^{1}H spin–lattice relaxation rates or by double-selective proton relaxation rates. ^{1}H–^{1}H dipole–dipole connectivities were observed in 2D NOE spectra and quantified by measuring absolute values of cross-relaxation rates or by fitting the experimental ^{1}H spin–lattice relaxation rates to a model of a sum of independent pairwise interactions. A molecular model was built showing extensive folding of the (phenylmethyl)-amino-ethyl chair and a chair conformation of the dihydropyridine moiety.

Nicardipine is a cerebral and coronary vasodilator drug with calcium blocking activity, structurally similar to nifedipine and nimodipine. Such 1,4-dihydropyridine derivatives, together with some diphenylalkylamines (e.g. verapamil) and benzothiazepines (e.g. diltiazem), belong to a general class of drugs interacting with the voltage-sensitive calcium channel and displaying a great variety of biological activities.

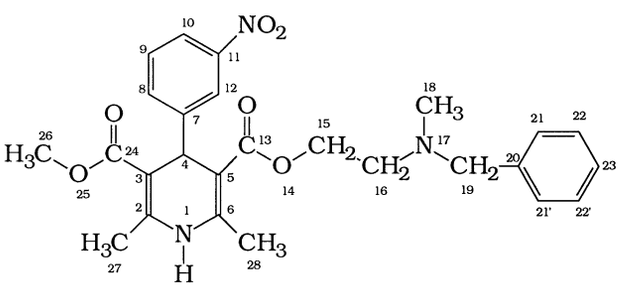

The diverse chemical structures and biological activities have attracted extensive research on molecular mechanisms of action as well as on conformational features in solution.[1–4]

In previous reports,[5–7] conformational features of nimodipine,[5] diltiazem[6] and verapamil[7] were delineated by using ^{1}H and ^{13}C NMR spectroscopy.

In this communication we report ^{1}H and ^{13}C NMR measurements on nicardipine in order to ascertain whether a change in substitutents may modulate the main conformational features of dihydropyridine calcium-channel blockers.

Experimental

Nicardipine (from Sandoz) was used without further purification. Solutions were made in deuterium oxide (99.95% from Merck) buffered at pH 6.2 with Na_2HPO_4 and NaH_2PO_4. NMR samples were carefully deoxygenated by sealing off the sample after several freezing–vacuum pumping–thawing cycles.

NMR spectra were carried out on a Varian VXR 200 Spectrometer operating at 4.7 T and on a Bruker AM 600 spectrometer operating at 14.1 T. The temperature was controlled to within ±1 K. Chemical shifts were referenced to internal [$^{2}H_4$]TSP (sodium trimethylsilylpropansulfonate). Spin–lattice relaxation rates (R_1) were measured with the inversion recovery pulse sequence. R_1 values were calculated with an exponential regression analysis of the recovery curves of longitudinal magnetisation components. Single- and double-selective proton spin–lattice relaxation rates were measured with inversion recovery pulse sequences modified to obtain single- or double-selective inversion of the desired proton resonances, as reported elsewhere.[8,9] All ^{1}H R_1 values were calculated in the initial rate approximation.[10]

2D ^{13}C–^{1}H shift correlated spectra were obtained in the gated decoupling mode by using standard pulse sequences. 2D NOE proton spectra were acquired with standard pulse sequences at mixing times, t_m, of 50–500 ms.

Molecular mechanics calculations were performed by using the MM+ forcefield through the MOBY software (Springer Verlag 1991) implemented on a 486 DX2/66 MHz PC.

Results

The ^{13}C NMR chemical shifts and spin-lattice relaxation rates are reported in Table 1. Spectral assignment was achieved by the attached proton test,[11] followed by selective decoupling experiments, and was verified by 2D ^{13}C–^{1}H shift correlated spectra. Effective motional correlation times modulating the corresponding one-bond ^{13}C–^{1}H dipolar interaction (also shown in Table 1) were calculated by Allerhand's formula.[12] The ^{13}C–{^{1}H} NOE values were measured with gated decoupling techniques and were found at the maximum value (1.98) for all protonated carbons.

^{1}H NMR parameters are summarised in Table 2. Spectral assignment was achieved by homonuclear spin decoupling and by reference to data in the literature. A comparison of non-selective, single-selective and double-selective proton spin-lattice relaxation rates of selected protons of nicardipine is reported in Table 3. The dipolar cross-relaxation rate of the corresponding proton pair, as calculated by the difference between the double selective and the single-selective rates, is also shown in the same Table.

Dipolar connectivities measured in 2D NOE proton spectra are schematised in Fig. 1 with no reference to their intensities. Normalised cross-peak areas were obtained by dividing the cross-peak volume at any value of the mixing time, t_m, by the volume of the corresponding diagonal peak measured at $t_m = 0$. These normalised intensities were analysed as a function of t_m, as shown in Fig. 2.

Table 1 150.9 MHz ^{13}C NMR parameters for nicardipine 10 mM in deuterium oxide buffered at pH 6.2 at 293 ± 1 K

Resonance	δ/ppm	R_1/s^{-1}	$\tau_{eff}10^{-10}$/s
C-13	171.5	0.17	—
C-24	169.6	0.52	—
C-7	151.6	0.57	—
C-11	150.6	0.20	—
C-3	149.2	0.59	—
C-5	149.1	0.75	—
C-8	135.8	3.20	1.58
C-21,21′	132.2	2.41	1.19
C-23	131.8	2.71	1.34
C-9	131.2	2.79	1.38
C-22,22′	130.9	2.08	1.03
C-20	130.4	0.63	—
C-12	123.5	2.89	1.43
C-10	123.3	4.45	2.20
C-2	103.5	0.40	—
C-6	101.2	0.72	—
C-19	61.7	3.60	0.89
C-15	60.0	8.13	2.01
C-16	55.7	3.80	0.94
C-18	53.1	1.27	0.21
C-26	41.7	1.15	0.19
C-4	40.4	3.18	1.57
C-27	19.8	1.21	0.20
C-28	19.6	1.34	0.22

Table 2 200 and 600 MHz ^{1}H NMR parameters for nicardipine 10 mM in deuterium oxide buffered at pH 6.2 at 293 ± 1 K

Resonance	δ/ppm	R_1^{200}/s^{-1}	R_1^{600}/s^{-1}
H-12	8.03	1.24	0.73
H-10	7.93	0.86	0.54
H-8	7.68	1.50	0.91
H-23	7.51	1.11	0.79
H-22,22′	7.48	1.16	0.82
H-9	7.44	1.51	0.87
H-21,21′	7.41	1.23	0.93
H-4	4.99	2.71	1.41
H-15	4.47	4.34	2.44
H-19a	4.22	3.12	2.38
H-19b	4.20	3.16	2.27
H-18	3.72	1.20	1.09
H-16	3.52	3.60	2.78
H-26	2.87	2.23	2.17
H-27	2.35	1.37	1.27
H-28	2.32	1.31	1.19

Discussion

The nucleus–nucleus dipolar interaction is the major source of structural information in NMR studies in solution. Dipolar connectivities are usually detected in 2D NOE spectra where the appearance of cross-peaks reveals the through-space interaction of nuclear spins. However, quantitative interpretation of such 2D maps is not straightforward and it is usually dealt with by computer programs that minimise the molecular model with the restraints provided by cross-peak approximated intensities. It is not a paradox that such programs work better for macromolecules where the number of input parameters is quite large. When dealing with medium size molecules the 2D map, such as that schematised in Fig. 1, contains few cross-peaks and several structures may be generated by the same input parameters.

An alternative approach is based on the interpretation of proton spin–lattice relaxation rates which are usually dominated by the ^{1}H–^{1}H dipole–dipole interaction. In a two spin-system such interaction yields the relaxation eqn. (1),[13] where ρ_i*

$$\frac{d}{dt}(I_{zi} - I_{0i}) = -(\rho_{ij} + \rho_i^*)(I_{zi} - I_{0i}) - \sigma_{ij}(I_{zj} - I_{0j}) \quad (1)$$

accounts for eventual contributions by relaxation mechanisms other than the dipole–dipole and ρ_{ij} and σ_{ij} are, respectively, the direct- and cross-relaxation rates that are differently contributed by the relaxation transition probabilities, eqns. (2) and (3),

$$\rho_{ij} = \frac{1}{10}\frac{\gamma_H^4\hbar^2}{r_{ij}^6}\left\{\frac{3\tau_{ij}}{1+\omega_H^2\tau_{ij}^2} + \frac{6\tau_{ij}}{1+4\omega_H^2\tau_{ij}^2} + \tau_{ij}\right\} \quad (2)$$

$$\sigma_{ij} = \frac{1}{10}\frac{\gamma_H^4\hbar^2}{r_{ij}^6}\left\{\frac{6\tau_{ij}}{1+4\omega_H^2\tau_{ij}^2} + \tau_{ij}\right\} \quad (3)$$

Table 3 200 MHz ^{1}H NMR non-selective (R^{nsel}), single-selective (R^{sel}), double-selective ($R_i^{i,j} \equiv$ rate measured for H-i after double-selective excitation of H-i and H-j) spin–lattice relaxation rates and dipolar cross-relaxation energies ($\sigma_{i,j}$) for selected protons of nicardipine 10 mM in deuterium oxide buffered at pH 6.2 at 293 ± 1 K

Resonance	R^{nsel}/s^{-1}	R^{sel}/s^{-1}	$R_i^{i,j}$/s^{-1}	$\sigma_{i,j}$/s^{-1}
H-12	1.24	0.92	$R_{12}^{12,4} = 1.05$	$\sigma_{12,4} = 0.13$
H-8	1.50	1.06	$R_8^{8,4} = 1.24$	$\sigma_{8,4} = 0.18$
H-4	2.71	1.91	$R_4^{4,8} = 2.11$	$\sigma_{4,8} = 0.20$
			$R_4^{4,12} = 2.05$	$\sigma_{4,12} = 0.14$
H-15	4.34	3.10	$R_{15}^{15,16} = 3.48$	$\sigma_{15,16} = 0.38$
H-16	3.60	2.57	$R_{16}^{16,15} = 2.99$	$\sigma_{16,15} = 0.42$

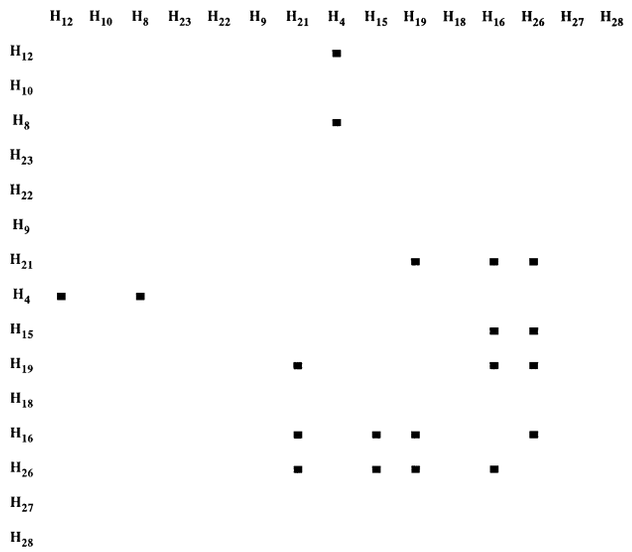

Fig. 1 Dipole–dipole connectivities observed in the 2D NOESY spectrum

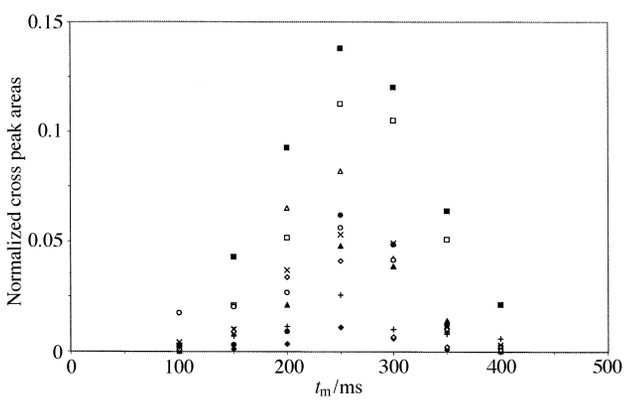

Fig. 2 Cross-peak intensities normalised to the intensity of the diagonal peak at $t = 0$ against the mixing time, t_m. ■ H16–H26; □ H19–H26; ▲ H16–H19; △ H15–H16; ● H15–H26; ○ H19–H21,21′; ◆ H16–H21,21′; ◇ H26–H21,21′; + H4–H8; × H4–H12.

where γ_H is the proton magnetogyric ratio, $\hbar$ is the reduced Planck constant ($\equiv h/2\pi$), r_{ij} is the internuclear distance, ω_H is the proton Larmor frequency and τ_{ij} is the correlation time typical of the motion that modulates the reorientation of the internuclear vector.

In a multispin system the relaxation equation is approximated by a sum of pairwise interactions extended to all the proton pairs, eqn. (4).

$$\frac{d}{dt}(I_{zi} - I_{0i}) = -\left(\sum_{j\neq i} \rho_{ij} + \rho_i^*\right)(I_{zi} - I_{0i}) - \sum_{j\neq i} \sigma_{ij}(I_{zj} - I_{0j}) \quad (4)$$

After the excitation pulse, the recovery of longitudinal magnetisation components is usually not a single exponential. However a spin–lattice relaxation rate is still defined in the initial rate approximation by eqn. (5). Such rate is labelled

$$R_i^{nsel} = \sum_{j\neq i} \rho_{ij} + \sum_{j\neq i} \sigma_{ij} + \rho_i^* \quad (5)$$

nsel (≡ nonselective) because the usual inversion recovery pulse sequences excite all the hydrogens belonging to the investigated molecule.

Two main problems must be faced whenever interpretation of proton spin–lattice relaxation rates is desired: (*i*) it must be ascertained that ρ_i^* can be effectively neglected and (*ii*) the reorientational dynamics at molecular level must be somehow delineated if r_{ij} values are desired. The distances obtained in this way represent proton–proton distances averaged among all the accessible molecular conformations.

The relevance of 'other' relaxation mechanisms can be evaluated by measuring the proton spin–lattice relaxation rates following any excitation profile that selectively affects only the chosen proton resonance, eqn. (6).

$$R_i^{sel} = \sum_{j\neq i} \rho_{ij} + \rho_i^* \quad (6)$$

Since the nonselective and the selective proton relaxation rates are differently contributed by the dipolar transition probabilities, the ratio between the two was suggested as a means of checking the relevance of ρ_i^*.[10] It is in fact consequent that such ratio is 1.5 in the case of a 100% contribution of the dipolar mechanism, provided the molecule reorientates within the extreme narrowing region ($\omega_H\tau_{ij} < 1$).

The experiments (Table 3) demonstrate that this holds for nicardipine in deuterium oxide where the values of R^{nsel}/R^{sel} are only slightly lower than 1.5 as a consequence of motional correlation times not well inside the extreme narrowing region and also of the experimental error.

As for the reorientational dynamics at molecular level a good piece of information is gained by ^{13}C NMR spin–lattice relaxation rates that are usually dominated by the one-bond (r = 1.09 Å)[14] ^{13}C–^{1}H dipole–dipole interaction. As a consequence isotropic motion determines equal normalised spin–lattice relaxation rates (R_1/n_H), where n_H is the number of attached protons for all protonated carbons and the motional correlation time, related to the isotropic rotational diffusion coefficient, can be evaluated by eqn. (7).[12]

$$R_1/n_H = 2.0235 \times 10^{10}\tau_R \quad (7)$$

When motional anisotropy and/or internal motions occur, which most probably applies to nicardipine in water solution, interpretation of spin–lattice relaxation rates in terms of rotational diffusion coefficients is not straightforward any longer, unless molecular motions are fitted to a well-defined physical model. However, eqn. (7) can still be applied even though what is obtained is a local or effective correlation time that has no relation with any rotational diffusion coefficient. From this point of view the data in Table 1 can be interpreted as follows. (*a*) Some internal motion occurs around the axis, since the spin–lattice relaxation rate of C-10 is rather slow if compared to those of C-8, C-9, C-12; (*b*) the correlation time for reorientation of the C-7–C-10 axis can be evaluated at 0.22 ns at 293 K from eqn. (7); (*c*) C-4 experiences a local mobility very similar to those experienced by the aromatic ring nearby, and the motional correlation time are in the range 0.14–0.16 ns at 293 K; (*d*) in contrast, internal motions do not apparently occur around any axis of the other aromatic ring where all protonated carbons relax at a rate very close to each other with a motional correlation time that can be calculated at 0.10–0.13 ns; (*e*) the C-15 methylene does not experience any additional degrees of motional freedom and it looks as if it is locked to the 1,4-dihydro-2,6-dimethyl-4-(3-nitrophenyl)-3,5-pyridinedicarboxylic acid moiety; whereas the other two methylenes (C-16 and C-19) reorient with a relatively short correlation time (*ca*. 0.09 ns) although without any indication of segmental motion; (*f*) all methyls behave as almost free rotors and are characterised by reorientational motions with quite short correlation times.

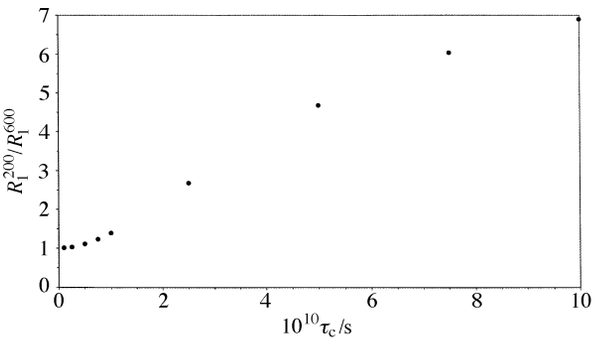

Fig. 3 Calculated ratio between the proton spin–lattice relaxation rates at 200 and 600 MHz against the motional correlation time

The values of correlation times obtained by spin–lattice relaxation rates of protonated carbons can be ratified by the frequency dependence of proton spin–lattice relaxation rates (Fig. 3). By inserting eqns. (2) and (3) into eqn. (5) upon the assumption of $\rho_i^* = 0$ and by considering the Larmor frequencies at the two used magnetic fields, eqn. (8) is in fact obtained.

$$\frac{R_1^{200}}{R_1^{600}} = \frac{\left\{\frac{3\tau_c}{1+\omega_{200}^2} + \frac{12\tau_c}{1+4\omega_{200}^2}\right\}}{\left\{\frac{3\tau_c}{1+\omega_{600}^2} + \frac{12\tau_c}{1+4\omega_{600}^2}\right\}} \quad (8)$$

The values obtained are in very good agreement with those already calculated, as exemplified for H-4 which yields a correlation time of 0.17 ns at 293 K.

Finally, if any two protons at a fixed distance are sufficiently resolved in the NMR spectrum, double-selective excitation of the two allows the calculation the corresponding dipolar cross-relaxation term from the difference, eqn. (9).[15]

$$\sigma_{ik} = R_i^{i,k} - R_i^{sel} = R_k^{i,k} - R_k^{sel} \quad (9)$$

Substitution of the known distance in eqn. (3) leads to a further evaluation of the local correlation time modulating the reorientation of the involved internuclear vector. This was accomplished for the H-19 geminal protons (r = 1.77 Å) yielding τ_c = 0.08 ns at 293 K, in very good agreement with the value obtained from ^{13}C relaxation rates.

With this dynamic picture in mind and also by considering the dipolar connectivities shown by the 2D NOE map, structural information may be gained in the following way.

Distances are first calculated for those proton pairs the σ_{ij} of which was measured by the double-selective relaxation technique by using the appropriate value of the correlation time. The data in Table 3 yield the following: (*a*) $r_{4,12} = 2.65$ and $r_{4,8} = 2.47$ Å with $\tau_{4,12} = \tau_{4,8} = 0.22$ ns at 293 K; (*b*) $\langle r_{15,16} \rangle = 2.77$ Å with $\tau_{15,16} = 0.22$ ns or $\langle r_{15,16} \rangle = 2.67$ Å with $\tau_{15,16} = 0.15$ ns which underlines the fact that the calculated distances are relatively free of the error that can be made by considering a value of correlation time.

The distance obtained in (*b*) is the average value among the four distances between each H-15 proton to each H-16 proton. In the minimised structure (*vide infra*), the four distances were $r_{15a,16a} = 3.07$, $r_{15a,16b} = 2.54$, $r_{15b,16a} = 2.38$, $r_{15b,16b} = 2.62$, which yields $\langle r_{15,16} \rangle = 2.67$ Å consistently with a motional correlation time shorter than the one modulating dipolar interactions in the 1,4-dihydro-2,6-dimethyl-4-(3-nitrophenyl)-3,5-pyridinedicarboxylic acid moiety.

The dipolar terms of proton pairs at any distance are then calculated by eqns. (2) and (3) upon substitution of a value of the local correlation time, as exemplified in Fig. 4 for $\tau = 0.14$ ns. With the list of these theoretical values the reconstruction of all the dipole–dipole interactions contributing to the observed relaxation pathway can be attempted and theoretical values of the spin–lattice relaxation rates can be obtained in a fairly good agreement with the experimental ones.

While the relaxation rates of H-10 and H-9 were suitably fitted by taking only the interaction with the vicinal proton into account, that of H-8 required consideration of the dipolar interaction with H-4 ($r = 2.65$ Å), as expected by 2D NOE maps and by double-selective experiments. However the H-12–H-4 interaction was not sufficient to fit the experimental value since it was yielding a relaxation rate of *ca*. 0.36 s^{-1}; as a consequence some additional contributions from protons located in other parts of the molecule were sought. The same was holding for H-21,21′ and H-22,22′, the relaxation rates of which were not completely accounted for by the interactions with the vicinal protons; moreover, the 2D NOE map strongly suggested folding back of the (phenylmethyl)aminoethyl ester chain; the two interactions between H-12 and one of the H-21,21′ protons and between H-12 and one of the H-22,22′ protons were therefore considered yielding an average distance of 2.78 Å for the two corresponding internuclear vectors. The relaxation rate of H-15 was satisfactorily fitted by the two interactions with H-16, that of H-16 was additionally contributed by interactions with H-19 and, finally, that of H-19 was contributed also by interactions with H-21,21′. All the distances used to account for the various relaxation terms are summarised in Table 4.

All obtained NMR parameters were used as restraints in molecular mechanics calculations where optimisation of the geometrical arrangement was carried out by using the MM+ force field. The obtained structure is shown in Fig. 5. This figure cannot be considered as showing the conformation assumed by nicardipine in water since molecular motions allow the molecule to assume several conformations separated by low energy gaps. What the figure shows is just a geometrical configuration as it emerges from motional averaging. It is, however, important to observe that folding back of the longer side chain is permitted as it was already hypothesised for nimodipine in Me_2SO.[5] It can be therefore concluded that calcium-channel blockers belonging to the dihydropyridine class are very likely to elicit their biological activity by assuming a conformation characterised by extensive folding of the side chain which leaves the basic nitrogen rather exposed and builds up a hydrophobic surface.

Table 4 Proton–proton distances (Å) used to calculate dipole–dipole relaxation terms considered in the fitting procedure of experimental spin-lattice relaxation rates of nicardipine 10 M in deuterium oxide buffered at pH 6.2 at 293 ± 1 K

	H-8	H-12	H-19	H-15
H-4	2.47	2.65		
H-21,21′		2.78	2.41	
			2.84	
H-22,22′		2.78		
H-16			2.24	3.07
			3.18	2.54
			2.70	2.38
			2.89	2.62

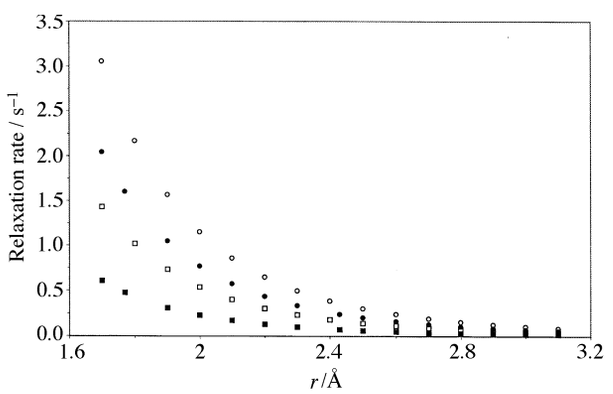

Fig. 4 Calculated direct- and cross-relaxation terms at 200 and 600 MHz against the proton–proton distance for an internuclear vector modulated by reorientational motions with $\tau_{eff} = 0.14$ ns. ○ *r* (200 MHz); □ *s* (200 MHz); ● *r* (600 MHz); ■ *s* (600 MHz).

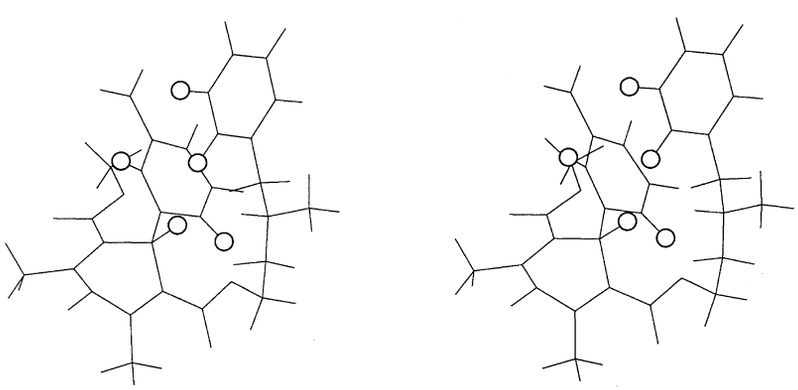

Fig. 5 Stereoview of the molecular model of the 'preferred' solution structure of nicardipine highlighting the protons considered to get restrained distances

References

1 S. H. Snyder and I. J. Reynolds, *New Eng. J. Med.*, 1985, **313**, 995.
2 A. M. Triggle, E. Shefter and D. J. Triggle, *J. Med. Chem.*, 1980, **23**, 1442.
3 R. Fossheim, K. Swarteng, A. Mostad, C. Romming, E. Shefter and D. J. Triggle, *J. Med. Chem.*, 1982, **25**, 126.
4 D. A. Langs and D. J. Triggle, *Mol. Pharmacol.*, 1985, **27**, 544.
5 E. Gaggelli, N. Marchettini and G. Valensin, *J. Chem. Soc., Perkin Trans. 2*, 1987, 1707.
6 A. Maccotta, G. Scibona, G. Valensin, E. Gaggelli, F. Botré and C. Botré, *J. Pharm. Sci.*, 1991, **80**, 586.
7 E. Gaggelli, A. Maccotta and G. Valensin, *J. Pharm. Sci.*, 1992, **81**, 367.
8 R. Freeman, *Chem. Rev.*, 1991, **91**, 1397.
9 E. Gaggelli and G. Valensin, *Concepts Magn. Reson.*, 1992, **4**, 339; 1993, **5**, 19.
10 R. Freeman, H. D. W. Hill, B. L. Tomlinson and L. D. Hall, *J. Chem. Phys.*, 1974, **61**, 4466.
11 C. LeCocq and J.-Y. Lallemand, *J. Chem. Soc., Chem. Commun.*, 1981, 150.
12 A. Allerhand, D. Doddrell and R. Komoroski, *J. Chem. Phys.*, 1971, **55**, 189.
13 J. H. Noggle and R. E. Schirmer, *The Nuclear Overhauser Effect*, Academic Press, New York, 1971.
14 K. Dill and A. Allerhand, *J. Am. Chem. Soc.*, 1979, **101**, 4376.
15 L. D. Hall and H. D. W. Hill, *J. Am. Chem. Soc.*, 1976, **98**, 1269.

Paper 6/03846*H*
Received 3*rd June* 1996
Accepted 24*th September* 1996